Available online at www.sciencedirect.com
SCIENCE DIRECT®
Computer Physics Communications 164 (2004) 262–268
Computer Physics Communications
www.elsevier.com/locate/cpc

Vlasov simulations of plasma-wall interactions in a weakly collisional plasma

G. Manfredi *, F. Valsaque [1]

Laboratoire de Physique des Milieux Ionisés et Applications, CNRS and Université Henri Poincaré, Faculté des Sciences et Techniques, BP 239, F-54506 Vandoeuvre-les-Nancy, France

Available online 27 July 2004

Abstract

An Eulerian Vlasov code is used to model plasma-wall interactions in a weakly collisional plasma. The different numerical methods used to solve the Vlasov and Poisson equations are described in detail. The code is used to simulate measurements of the ion distribution and ion temperature in a low-pressure argon plasma. In particular, it is shown that the presence of material walls can lead to significant errors in the measurements, if the effect of the sheaths is not properly taken into account.

PACS: 52.65.-y; 52.40.Hf; 52.25.Dg

Keywords: Plasma kinetic simulations; Vlasov codes; Weakly collisional plasmas; Argon discharge

1. Introduction

A detailed understanding of plasma-wall interactions is of paramount importance in a large number of problems of practical interest. This is hardly surprising, as any plasma created in the laboratory needs to be confined by a material vessel. In tokamak plasmas, for example, material structures such as limiters and divertors are eroded by the impact of energetic ions, thus generating impurities (i.e., high Z neutral atoms) by physical sputtering. Such impurities may be ionized in the scrape-off layer and transported into the core, where they degrade the plasma confinement [1].

Another application of plasma-wall interactions concerns the interpretation of probe measurements [2]. Indeed, a large variety of diagnostics are obtained with probes inserted into the plasma, thus exposing some solid surface to the charged particles. It is well known that such probe-plasma interaction alters the plasma parameters in the vicinity of the probe, and may lead to significant errors in the measurements.

Perhaps the most important effect caused by the presence of a solid surface is the formation of plasma sheaths. Indeed, ions and electrons hit the surface at very different rates, roughly proportional to their thermal speeds (for equal temperatures, the electron thermal speed is about forty times that of hydrogen ions). If the surface is an insulator, or kept electrically isolated, a net charge develops on it and perturbs the

* Corresponding author.
E-mail address: giovanni.manfredi@lpmi.uhp-nancy.fr (G. Manfredi).
[1] Present address: Laboratoire de Chimie du Solide Minéral, CNRS UMR 7555, Université Henri Poincaré, BP 239, F-54506, Vandoeuvre-lès-Nancy, France.

0010-4655/$ – see front matter
doi:10.1016/j.cpc.2004.06.037

ambient electric field, the ion temperature and current, as well as other crucial parameters. This perturbation of the plasma, characterized by the presence of a distinct space charge, is called the Debye sheath (DS). The DS is crucial in mediating the transition from the unperturbed plasma to the wall, but cannot be directly connected to the unperturbed plasma. It must be preceded by a quasineutral region, the presheath (PS), which is dominated by collisions and/or ionization, whereas the DS is essentially collisionless (in more complex cases, the PS may also be determined by geometrical or magnetic effects [3]).

In this paper, we shall propose a kinetic model for plasma-wall interactions, which is capable of describing both the collisionless DS and the collisional PS. The numerical techniques used to solve this model will also be described. Finally, the model will be applied to the physics of plasma-wall interactions in a low-pressure argon plasma.

2. Model

Numerical and analytical studies of plasma-wall interactions have frequently been performed using fluid models for the ions, and assuming thermal equilibrium for the electrons (see, for instance, Ref. [3]). Pioneering results with a collisionless kinetic model and particle-in-cell (PIC) simulations were obtained by Chodura [4] for a magnetized plasma. In the present paper, we include collisional effects, though we restrict ourselves to the case of an unmagnetized plasma (or a magnetic field normal to the surface, which amounts to the same). Therefore, we are able to model the entire transition region (DS and PS), from the unperturbed Maxwellian plasma to the wall surface.

For a correct description of the presheath, the model will have to include collisions and ionization, at least in a simplified form. The ion Vlasov equation is thus supplemented with a collision term of the Bhatnagar–Gross–Krook (BGK) type, which models the relaxation of the ion population towards the equilibrium Maxwellian $f_0(v)$ with a typical rate equal to ν [5]. In one dimension, the resulting kinetic equation reads as:

$$\frac{\partial f_i}{\partial t} + v\frac{\partial f_i}{\partial x} - \frac{e}{m_i}\frac{\partial \phi}{\partial x}\frac{\partial f_i}{\partial v} = -\nu(f_i - f_0), \tag{1}$$

where x is the coordinate normal to the wall and v the corresponding velocity; ϕ is the electrostatic potential; $e > 0$ and m_i are respectively the ion charge and mass and $f_i(x, v, t)$ is the ion distribution function in phase space.

Eq. (1) is coupled to Poisson's equation, where the electron density is given by the Boltzmann relation and $n_i(x, t) = \int f_i \, dv$:

$$\frac{\partial^2 \phi}{\partial x^2} = -\frac{e}{\varepsilon_0}\left[n_i - n_0 \exp(e\phi/k_B T_e)\right]. \tag{2}$$

Here, ε_0 is the vacuum dielectric constant, k_B is Boltzmann's constant, T_e is the electron temperature and n_0 is the equilibrium ion and electron density in the unperturbed plasma.

Appropriate boundary conditions are chosen. At $x = 0$ (position of the perfectly absorbing wall) ions are allowed to leave the system, and no incoming flux exists; at $x = L$ (plasma core) the ion distribution is kept fixed and equal to that of the equilibrium plasma, with given temperature T_{i0} and density n_0.

For Poisson's equation, we take $\phi = 0$ in the plasma ($x = L$), whereas the wall is assumed to be at the floating potential given by the accumulation of electric charges on the wall itself. The floating potential is computed by integrating Ampère's equation on the wall ($x = 0$):

$$\frac{\partial E}{\partial t} = -e(j_i - j_e)/\varepsilon_0, \tag{3}$$

where $E = -\partial\phi/\partial x$ is the electric field. The ion flux is given by: $j_i = \int v f_i \, dv$. The electron flux is estimated by assuming that the electron velocity distribution is half-Maxwellian on the wall, which yields:

$$j_e(0, t) = n_0\left(\frac{k_B T_e}{2\pi m_e}\right)^{1/2} \exp\left(\frac{e\phi(0)}{k_B T_e}\right). \tag{4}$$

The BGK term on the r.h.s. of Eq. (1) acts as a sink/source term, whose effect is to reconstruct the equilibrium Maxwellian on a time scale of order ν^{-1}. Physically, it is supposed to model ion-neutral collisions and ionization, f_0 representing the equilibrium ion distribution far from the wall. Although very simple, this model contains enough physics to describe the transition between the equilibrium plasma and the wall, and has the advantage of depending on a single free parameter, namely the collision frequency ν

(or equivalently the mean-free-path $\lambda = v_{thi}/\nu$, where $v_{thi} = \sqrt{k_B T_{i0}/m_i}$ is the ion thermal speed).

In this paper, we shall only be interested in the equilibrium solutions of this model. In order to obtain such solutions, we first initialize the distribution function to be equal to the equilibrium Maxwellian f_0; then, we let it evolve according to our model equations until a stationary state appears. As we are not interested in the time-dependent transient, there is no need for a very accurate timestepping technique, as long as the final state is recovered correctly. This point will affect our choice of the numerical techniques, as detailed in the following section.

3. Numerical methods

3.1. Vlasov and Poisson's equations

The ion Vlasov equation is integrated numerically using an Eulerian code, which solves the kinetic equation on a fixed phase space grid. The main advantage of Eulerian codes is their lack of random statistical noise, inherent to particle-in-cell calculations, which renders them accurate even in regions of the phase space where the plasma is dilute (this is the case, for instance, in the DS, where the ion density decreases significantly).

The timestepping technique is based on a splitting algorithm [6], which amounts to solving, for each timestep, first the free-streaming part of Eq. (1): $\partial_t f_i + v\partial_x f_i = 0$, then the term containing the electrostatic field: $\partial_t f_i + (eE/m_i)\partial_v f_i = 0$, and finally the BGK collision term: $\partial_t f_i = -\nu(f_i - f_0)$. The solution from time t_n to time t_{n+1} can thus be obtained in three steps:

$$f^\star(x,v) = f(x - v\Delta t, v, t_n), \tag{5}$$

$$f^{\star\star}(x,v) = f^\star(x, v - eE\Delta t/m_i), \tag{6}$$

$$f(x,v,t_{n+1}) = f^{\star\star}(x,v) - \nu\Delta t\big[f^{\star\star}(x,v) - f_0(v)\big], \tag{7}$$

where $f^\star$ and $f^{\star\star}$ denote intermediate solutions. We see that the standard Vlasov terms give rise to constant shifts in either position or velocity space (Eqs. (5) and (6)). In their numerical implementation, these shifts require the interpolation of the distribution function in phase space, which is performed here using a finite-volume technique described in Ref. [7]. The collisional term has an algebraic solution that requires no interpolation.

The resulting numerical scheme is only first order accurate in time, but this is not too important as we are not trying to describe the time-dependent transient. In practice, we start with a relatively large timestep in order to roughly approach the final stationary solution, then decrease it several times to obtain a more accurate result.

Poisson's equation is nonlinear because of the exponential Boltzmann factor appearing in the electron density. We integrate it by using an iterative method combined with centered differences to represent the second derivative:

$$\begin{aligned}&\big(\phi_{j+1}^{s+1} - 2\phi_j^{s+1} + \phi_{j-1}^{s+1}\big) - \alpha\phi_j^{s+1}\\ &\quad = -\frac{e\Delta x^2}{\varepsilon_0}\big[n_{i,j} - n_0\exp(e\phi_j^s/k_B T_e)\big] - \alpha\phi_j^s,\end{aligned} \tag{8}$$

where the subscript j indicates the grid point, and the superscript s the iteration step. Notice that, without the term proportional to α on both sides of Eq. (8), this iterative procedure would not be convergent. Various tests have shown that the fastest convergence is obtained for $\alpha \simeq \Delta x^2/\lambda_{De}^2$. The initial guess for the iterative procedure is taken to be the potential at the previous timestep. As the potential varies little from one timestep to the next, this is rather a good guess, which allows the method to converge in about 20 iterations.

3.2. Non-uniform mesh

The model described in Section 2 is valid for a weakly collisional plasma, where the mean-free-path is much larger than the Debye length. In this case, the size of the PS, which scales as the mean-free-path, is much larger than the size of the DS, which is only a few Debye lengths thick. Furthermore, steep spatial gradients are generally present in the DS, whereas all quantities vary much more smoothly in the PS.

We are therefore confronted with a two-scale problem: a uniform mesh that resolves the DS scale would waste a lot of mesh points in the PS. In order to distribute mesh points in a more sensible way, we resort to a non-uniform grid [8] by introducing the new position variable z through the relation

$$x = z^\delta, \quad \delta > 1. \tag{9}$$

Differentiating Eq. (9) we obtain: $\Delta x = \delta z^{\delta-1}\Delta z$. If the mesh points are regularly spaced in the z variable (i.e., $\Delta z = \text{const.}$), then the mesh size in real space Δx will be smaller near the wall (located at $x = 0$) and larger further from the wall. This simple trick enables us to concentrate mesh points in the DS region.

However, the change of variable defined in Eq. (9) modifies both the Vlasov and Poisson's equations, so that the numerical techniques described earlier may need to be modified. The transformed Poisson's equation becomes:

$$z\frac{\mathrm{d}^2\phi}{\mathrm{d}z^2} + (1-\delta)\frac{\mathrm{d}\phi}{\mathrm{d}z} = -\frac{e}{\varepsilon_0}\delta^2 z^{2\delta-1}\left[n_i(z) - n_0\exp\left(e\phi(z)/k_B T_e\right)\right]. \tag{10}$$

Eq. (10) can be solved by means of an iterative method completely analogous to the one described earlier for the standard Poisson's equation.

Things are slightly more complex for the transformed Vlasov equation, which reads as:

$$\delta z^{\delta-1}\frac{\partial f_i}{\partial t} + v\frac{\partial f_i}{\partial z} - \frac{e}{m_i}\frac{\partial\phi}{\partial z}\frac{\partial f_i}{\partial v} = -\delta z^{\delta-1}\nu(f_i - f_0). \tag{11}$$

Unfortunately, the splitting technique detailed in the previous paragraph would not work well for the transformed Vlasov equation (11). The reason is that, in the free-streaming term, the effective velocity becomes $v/(\delta z^{\delta-1})$, which is position-dependent. Therefore the shift-like solution described in Eq. (5) would not be correct, and the numerical scheme would have to be significantly modified [9].

Instead, our strategy is to replace Eq. (11) with the following equation:

$$\frac{\partial f_i}{\partial t} + v\frac{\partial f_i}{\partial z} - \frac{e}{m_i}\frac{\partial\phi}{\partial z}\frac{\partial f_i}{\partial v} = -\delta z^{\delta-1}\nu(f_i - f_0). \tag{12}$$

The point is that both Eqs. (11) and (12) possess the *same stationary solutions*, although of course not necessarily the same time-dependent transient. As we are only interested in the stationary states, we solve Eq. (12), for which the standard Vlasov code can be directly applied (indeed only the collisional term is slightly changed, but this is straightforward to implement in the code). In practice, this amounts to solving a Vlasov equation containing a BGK term with a position-dependent effective collision rate $\nu^\star(z) = \delta z^{\delta-1}\nu$.

4. Simulations of a low-pressure argon plasma

This section illustrates an application of the Vlasov kinetic code described previously. We consider a low-pressure argon plasma confined in a cylindrical magnetic multipolar device, as studied experimentally by Bachet et al. [10,11]. Their apparatus was especially designed to measure the ion temperature with the help of a laser induced fluorescence (LIF) diagnostic. The main interest of a spectroscopy diagnostic is to provide valuable information without perturbing the medium that is being measured. Like all experimental results, however, spectroscopic measurements need to be carefully assessed and interpreted, and a failure to do so may lead to an incorrect estimation of the measured quantities.

In the experiment described here [11], LIF measurements near an electrically floating wall yielded values of the ion temperature above 2 eV. This is clearly an overestimation, as the ion temperature in the plasma core is known to be only 0.05 eV, and even the electron temperature does not exceed 2 eV. The origin of this incorrect measurement of the ion temperature is, however, not completely clear. The scope of our simulations is to suggest a physical explanation for such an overestimation [12].

4.1. Experimental setup and simulation model

Bachet and co-workers [11] produced an argon plasma at 6×10^{-4} Torr in a cylindrical vessel, 45 cm in diameter and 80 cm long, bounded at each end by an electrically floating wall (Fig. 1). By restricting our study to the region along the cylinder axis (named x axis hereafter), we can assume that the lateral surface of the cylinder is sufficiently distant not to influence the plasma behavior. In this case, the problem can be reduced to that of a one-dimensional plasma bounded by two walls [3,8]. Due to the symmetry of the vessel (Fig. 1), we can further simplify the geometry of the problem by considering only half of the cylinder between $x = 0$ (the wall) and $x = L = 40$ cm (the plasma core).

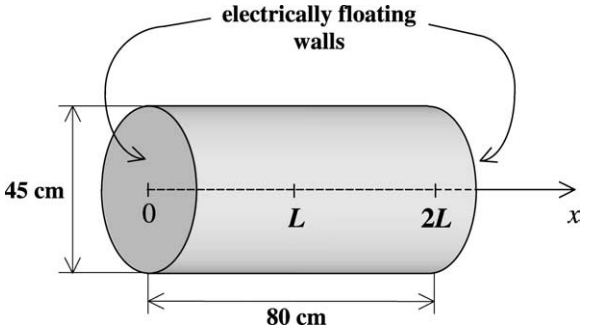

Fig. 1. Geometry of the experimental setup used by Bachet et al. [10,11].

Under the conditions of the experiment, the ion–ion, the ion–electron, and the ion-neutral mean-free-paths are respectively: $\lambda_{ii} \sim 10^4$ cm, $\lambda_{ie} \sim 10^6$ cm, and $\lambda_{in} \sim 12$ cm [11,13]. By comparing these typical lengths with the size of the cylinder ($L = 40$ cm), it is clear that only ion-neutral collisions need to be taken into account. Moreover, as $\lambda_{in} = 0.3L$, the ions created in the plasma core undergo only a few collisions before reaching the wall. The plasma is therefore weakly collisional, and it is appropriate to describe the ion dynamics by means of a Vlasov equation (1), supplemented by a BGK collision term with the collision frequency ν given by v_{thi}/λ_{in}.

As detailed in Section 2, the self-consistent electric potential is computed from Poisson's equation (2), where we assume Boltzmann electrons with uniform temperature $T_e = 1.8$ eV and core density $n_e(x = L) = n_0 = 10^9$ cm^{-3} [11]. We postulate a perfectly absorbing wall located at $x = 0$, so that all ions reaching the wall are lost. At $x = L$, the ion distribution is kept fixed and equal to that of the plasma core: $f_i(x = L, v) = f_0(v)$, where f_0 is a Maxwellian with temperature $T_{i0} = 0.05$ eV and density $n_i(x = L) = n_0 = 10^9$ cm^{-3} [11].

Our aim is to compute the stationary solution of Eqs. (1), (2), which is supposed to be unique. As explained in Section 2, our procedure is to initialize the system with a spatially homogeneous initial condition $f_i(x, v, t = 0) = f_0(v)$, then let it evolve under the action of Eqs. (1), (2) until a self-consistent stationary solution has emerged. The results presented in the next paragraphs refer to the sheath structure for such a stationary state.

4.2. Sheath structure and ion temperature estimation

Fig. 2 shows the ion and electron density profiles in the left-hand half of the cylinder (see Fig. 1). The density profiles clearly display two very different scales of spatial variation: the Debye length $\lambda_{De} = 0.32$ mm (computed with n_0 and T_e) and the ion-neutral mean-free-path $\lambda_{in} \sim 12$ cm. These scales define respectively the non-neutral Debye sheath (DS) and the quasi-neutral presheath (PS). The boundary between the DS and the PS seems to be around $x = 3$–4 mm. In order to describe correctly this two-scale problem without using an excessive number points in the spatial direction, we have employed a non-uniform mesh (as described in Section 3.2). An accurate spatial

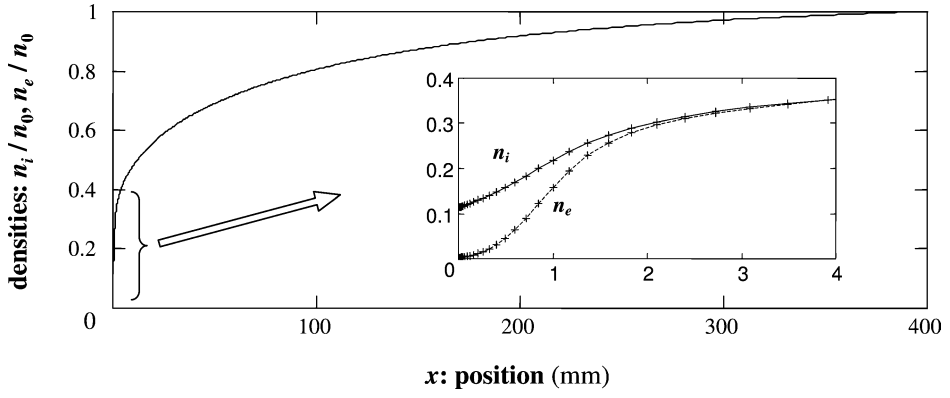

Fig. 2. Ion and electron density profiles (solid and dashed curves respectively) in the left-hand half of the cylinder. The inset shows an enlargement of the density profiles near the electrically floating wall, located at $x = 0$. The crosses indicate the mesh points of the non-uniform spatial mesh used in the Vlasov simulation.

mesh throughout the DS and the PS was obtained with $\delta = 4$ and 400 points.

Due to presence of a significant space charge, a strong electric field exists in the DS, which accelerates the ions towards the wall and creates a shear in their velocity distribution. This is well illustrated by Fig. 3(a), which shows several cuts of the phase space distribution at different positions [in this figure, all distributions $f_i(v)$ are renormalized so that they have the same maximum]. Note that within the DS, the ion velocity distribution varies rapidly over a distance of a few millimeters.

Furthermore, even though the ions are Maxwellian in the plasma core, their velocity distributions near the wall are clearly not Maxwellian. This fact points out that a kinetic model is indeed necessary for an accurate description of the plasma-wall transition, as most fluid models do not take into account any departure from the Maxwellian distribution. For a non-Maxwellian distribution, the temperature is not precisely defined. In such situations, most authors [1,4,14] define it as a quantity proportional to the standard deviation of the distribution: $T_i = \frac{m_i}{n_i k_B} \int (v - \langle v \rangle)^2 f_i \, dv$ ($\langle v \rangle$ is the average velocity), which coincides with the thermodynamic temperature for a Maxwellian distribution.

At 10 mm from the wall, it is found that the LIF and simulation results yield similar values for the ion temperature, respectively 0.24 eV [11] and 0.20 eV. On the contrary, at 1 mm from the wall, the simulation result is $T_i = 0.08$ eV, whereas the LIF measurement is $T_i = 2.26$ eV [11]. As explained earlier, such an exceptionally large value of the ion temperature obtained by LIF is most probably incorrect for this type of low-pressure plasma (it is even higher than the electron temperature $T_e = 1.8$ eV).

Our interpretation of this over-estimation relies on the shearing effect mentioned above. Fig. 3(a) shows that the velocity distribution profiles vary significantly between $x = 0$ and $x = 3$ mm from the wall (that is, within the DS). But the spatial resolution of the LIF diagnostic is of about 6 mm^3 [10], which roughly corresponds to a resolution of 2 mm in one dimension. Therefore, the LIF measurement at, for example, $x = 1$ mm from the wall does not provide the actual shape of the ion distribution, but rather an average (or convolution) of the distribution profiles between $x = 0$ and $x = 2$ mm. It is obvious from Fig. 3(a) that such an averaged distribution should be considerably wider in velocity space, and thus yield a larger (and overestimated) value of the ion temperature.

In order to check the reliability of this interpretation, we plot in Fig. 3(b) the velocity distribution profiles (at different positions) averaged over 2 mm. The average is performed by convolution with a step function that has a width of 2 mm. At $x = 1$ mm, the averaged velocity profile is much wider than the non-averaged one (Fig. 3(a)). The kinetic temperature deduced from the averaged velocity distribution is approximately $T_i \simeq 0.8$ eV, which is ten times larger than the simulated ion temperature from the raw distribution, but still smaller than the experimental value $T_i = 2.26$ eV [11]. However, the temperature given in Ref. [11] was not computed with the simple formula

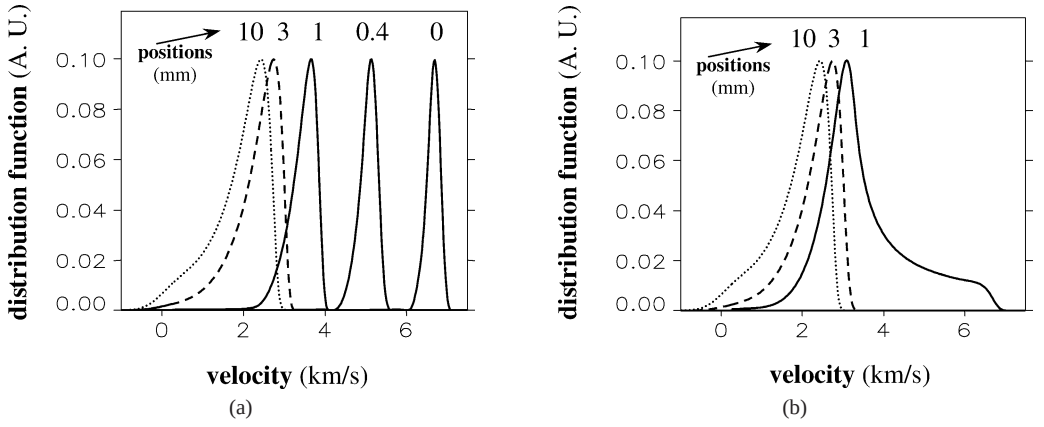

Fig. 3. Profiles of the ion velocity distribution $f_i(v)$ at different positions. All profiles have been normalized so that they have the same maximum. (a) Raw distributions from the Vlasov simulation; (b) averaged distributions.

given in the previous paragraph (standard deviation of the velocity distribution), but rather using a more complex model due to Emmert et al. [8]. A direct comparison of the temperatures is thus not meaningful. But comparing the experimental profile [11] with the numerical profile (after convolution) shows a remarkable agreement, both in the shape and in the width of the distributions. This agreement indicates that the overestimated LIF temperature is indeed due to the spatial variation of the ion distribution in the DS, which occurs on a scale shorter than the resolution of the diagnostic.

At 10 mm from the wall (which is beyond the DS and well into the PS), the averaging procedure leaves the velocity distribution virtually unaffected (see Figs. 3(a) and 3(b)). This is because the ion distribution varies much more smoothly in the PS, so that the finite resolution of the diagnostic does not affect the measurement.

In summary, we have shown that ion temperature measurements obtained from LIF diagnostics are not accurate in the DS, because the typical length of spatial variations (the Debye length, $\lambda_{De} \simeq 0.32$ mm) is in this case smaller than the resolution of the diagnostic, which is approximately 2 mm. This problem does not exist in the PS, where spatial variations of the ion distribution function are much smoother.

5. Conclusion

We have presented a one-dimensional Vlasov–Poisson model for the treatment of weakly collisional plasmas. The Vlasov equation is supplemented by a BGK collision term, so that the model is capable of describing the entire plasma-wall transition, including both the Debye sheath and the presheath. Although simple, this model has already been shown to be appropriate to describe the interaction of a probe (retarding field analyzer) with a strongly magnetized plasma in a tokamak edge [2]. In the present work, the BGK term models ion-neutral collisions and ionization in a low-pressure argon plasma. The Vlasov Eulerian code used to solve the kinetic equation allowed us to obtain fine-resolution results for the ion distribution function, from which accurate estimations of the ion temperature could be inferred. These were compared to the experimental results of Ref. [11], which displayed abnormally large values of the ion temperature near an electrically floating wall. Our analysis of the ion distribution function enabled us to detect the origin of such overestimated temperature measurements, which are due to the rapid ion acceleration in the Debye sheath.

Acknowledgements

We thank F. Doveil and G. Bachet for many helpful discussions on the experimental setup.

References

[1] P.C. Stangeby, The Plasma Boundary of Magnetic Fusion Devices, Institute of Physics Publishing, London, 2000.
[2] F. Valsaque, G. Manfredi, J.P. Gunn, E. Gauthier, Phys. Plasmas 9 (2002) 1806.
[3] K.-U. Riemann, J. Appl. Phys. D 24 (1991) 493.
[4] R. Chodura, Phys. Fluids 25 (1982) 1628.
[5] F. Valsaque, G. Manfredi, J. Nucl. Materials 290–293 (2001) 763.
[6] C.Z. Cheng, G. Knorr, J. Comput. Phys. 22 (1976) 330.
[7] E. Fijalkow, Comput. Phys. Commun. 116 (1999) 319.
[8] G.A. Emmert, R.M. Wieland, A.T. Mense, J.N. Davidson, Phys. Fluids 23 (1980) 803.
[9] E. Sonnendrucker, J. Roche, P. Bertrand, A. Ghizzo, J. Comput. Phys. 149 (1999) 201.
[10] G. Bachet, L. Chérigier, M. Carrère, F. Doveil, Phys. Fluids B 5 (1993) 3097.
[11] G. Bachet, L. Chérigier, F. Doveil, Phys. Plasmas 2 (1995) 1782.
[12] F. Valsaque, PhD thesis, University of Nancy, France, 2002.
[13] L. Chérigier, PhD thesis, University of Marseille, France, 1994.
[14] K.-S. Chung, I.H. Hutchinson, Phys. Rev. A 38 (1988) 4721.